PROTEINS: Structure, Function, and Genetics 45:183–189 (2001)

Successful Molecular Dynamics Simulation of Two Zinc Complexes Bridged by a Hydroxide in Phosphotriesterase Using the Cationic Dummy Atom Method

Yuan-Ping Pang*

Mayo Clinic Cancer Center, Department of Molecular Pharmacology and Experimental Therapeutics, Tumor Biology Program, Molecular Neuroscience Program, Mayo Clinic, Rochester, Minnesota

ABSTRACT **I report herein two 2.0 ns (1.0 fs time step) MD simulations of two zinc complexes bridged by a hydroxide in phosphotriesterase (PTE) employing the nonbonded method and the cationic dummy atom method that uses virtual atoms to impose orientational requirement for zinc ligands. The cationic dummy atom method was able to simulate the four-ligand coordination of the two zinc complexes in PTE. The distance (3.39 ± 0.07Å) between two nearby zinc ions in the time-average structure of PTE derived from the MD simulation using the cationic dummy atoms matched that in the X-ray structure (3.31 ± 0.001Å). Unequivocally, the time-average structure of PTE was able to fit into the experimentally determined difference electron density map of the corresponding X-ray structure. The results demonstrate the practicality of the cationic dummy atom method for MD simulations of zinc proteins bound with multiple zinc ions. In contrast, a 2.0 ns (1.0 fs time step) MD simulation using the nonbonded method revealed a striking difference in the active site between the X-ray structure and the time-average structure that was unable to fit into the density map of PTE. The results suggest that caution should be used in the MD simulations using the nonbonded method. Proteins 2001;45:183–189.** © 2001 Wiley-Liss, Inc.

Key words: coordination chemistry; metalloproteins; metal–metal interactions; molecular dynamics; zinc

INTRODUCTION

Zinc proteins are biologically important. They include zinc fingers as transcription factors,[1] endostatin,[2] and matrix metalloproteins[3–5] that are involved in cancers and cardiovascular diseases, and zinc proteases as lethal factors in anthrax[6] and botulinum toxins.[7] A long-standing problem with molecular dynamics (MD) simulations of zinc proteins is that the four-ligand coordination of zinc identified in X-ray structures is changed to six-ligand coordination during MD simulations.[8] Two general methods have been reported for solving the problem in MD simulations of zinc proteins. The first one termed the *bonded* model uses covalent bonds between zinc and its coordinates to maintain the four-ligand coordination in proteins during MD simulations.[9–11] The second termed the *nonbonded* model (thereafter model A) maintains the four-ligand coordination with the electrostatic and van der Waals forces to avoid the use of covalent bonds that are restrained with a harmonic potential and inevitably freeze the zinc-containing region in proteins.[12–16] Recently, it has been reported that an MD simulation with a semiempirical quantum-chemical description (MNDO/d) of a zinc core in metalothionein-2 is able to give correct zinc complex geometries and an overall protein structure in agreement with the corresponding experimentally determined structures, although the simulation is more computationally expensive than classical MD simulations.[17] I have reported a simple method, termed the *cationic dummy atom* model (thereafter model B), which is successful in simulating the four-ligand coordination of zinc without the use of covalent bonds between zinc and its ligands in nanosecond-length MD simulations of four zinc proteins with which the MD simulations using model A failed.[8,18] Technically akin to the *seven-electrostatic-center* approach proposed for modeling transition-metal ion,[19] model B uses four identical dummy atoms tetrahedrically attached to the zinc ion and transfers all the atomic charge of the zinc divalent cation evenly to the four dummy atoms (Fig. 1). The four peripheral atoms are "dummy" in that they interact with other atoms electrostatically but not sterically. Therefore, the cationic dummy atoms effectively mimic zinc's $4s4p^3$ vacant orbitals that accommodate the lone-pair electrons of zinc coordinates[20] thus imposing the requisite orientational requirement for zinc coordinates and simulating zinc's propensity for the four-ligand coordination.[18]

To evaluate the practicality of model B for MD simulations of zinc proteins, especially those bound with multiple zinc ions, it is desirable to perform nanosecond-length MD simulations of the crystal structure of phosphotriesterase (PTE) liganded with two zinc ions and diethyl 4-methylbenzylphosphonate (DMP) using models A and B, respectively, to investigate if model A or B or both can simulate the four-ligand coordination of the two zinc ions in PTE,

Grant sponsor: Mayo Foundation.

*Correspondence to: Yuan-Ping Pang, Guggenheim 711A, Mayo Clinic, 200 First Street SW, Rochester, MN 55905. E-mail: pang@mayo.edu

Received 23 February 2001; Accepted 28 June 2001

and to compare the accuracy of the two models by crystallographic analyses of the time-average structures derived from MD simulations. The use of the PTE complex in this study was because the two zinc ions in the active site of PTE were bridged by one hydroxide ion,[21,22] which offered an excellent opportunity to test the zinc force field parameters for not only the intermolecular interactions between the zinc ion and the protein residues but also the intermolecular interaction between the two nearby zinc ions. An additional reason was because a 550 ps (2.0 fs time step) MD simulation of the DMP-PTE complex using model A had been reported,[22] which offered direct comparison of the 550 ps MD simulation with nanosecond-length MD simulations using models A and B, respectively.

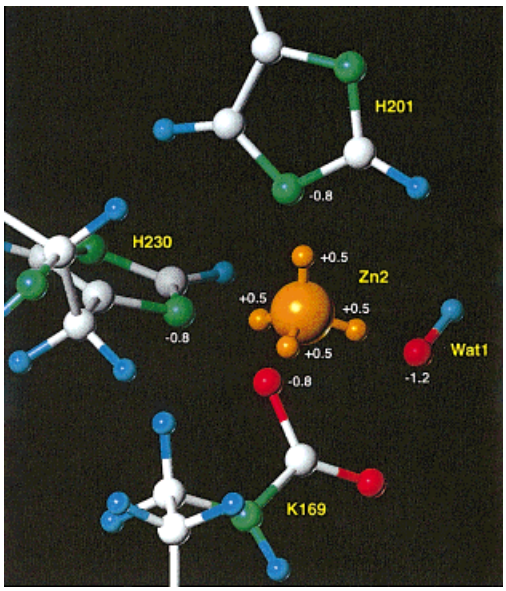

Fig. 1. A close-up view of the zinc divalent cation attached with four cationic dummy atoms used in the MD simulation of the DMP-PTE complex showing the atomic charges on the dummy atoms and zinc ligands (green = N; white = C; red = O; cyan = H; and orange = Zn).

METHODS

DMP-PTE Complex

The initial structure of the DMP-PTE complex, including two zinc divalent cations, one hydroxide (labeled with Wat1), and 67 crystallographically determined water molecules buried inside the protein, used in all MD simulations was taken from the second subunit (segment B) of the corresponding X-ray structure (PDB code: 1DPM).[23] Two types of protonation states of zinc ligands were used in this study. Type I used two neutral and two anionic zinc ligands for each zinc ion in PTE (Zn1: OH^{-1}, $D^{-1}301$, H55, and H57; Zn2: OH^{-1}, $Lyx^{-1}169$, H201, and H230) whereas type II used four anionic zinc ligands for each zinc ion in PTE (Zn1: OH^{-1}, $D^{-1}301$, $H^{-1}55$, and $H^{-1}57$; Zn2: OH^{-1}, $Lyx^{-1}169$, $H^{-1}201$, and $H^{-1}230$) according to the hypothesis of histidinate as zinc ligand in proteins recently reported in the literature.[8,21,24] In the PTE structure with protonation of type I, H254 was protonated; H55, H57, and H230 were neutral and carried a proton attached to the delta nitrogen atom of the imidazole ring; H123, H201, and H257 were neutral and carried a proton attached to the epsilon nitrogen atom; all R and K residues, E56, D100, and D105 were protonated; all other E and D residues were deprotonated; R36, R88, R89, R91, R164, R225, R356, K339, D235, D236, E263, and E71 were each neutralized by Cl^- or Na^+; and the water molecule (Wat1) coordinating with the two zinc divalent ions was deprotonated.[21,22] The RESP charges of the H and O atoms of Wat1 were +0.2049 and −1.2049, respectively. In the PTE structure with protonation of type II, H55, H57, H201, and H230 were treated as histidinate;[8,21,24] D253 was protonated;[24] D208 and H201 were each neutralized by Na^+; and the

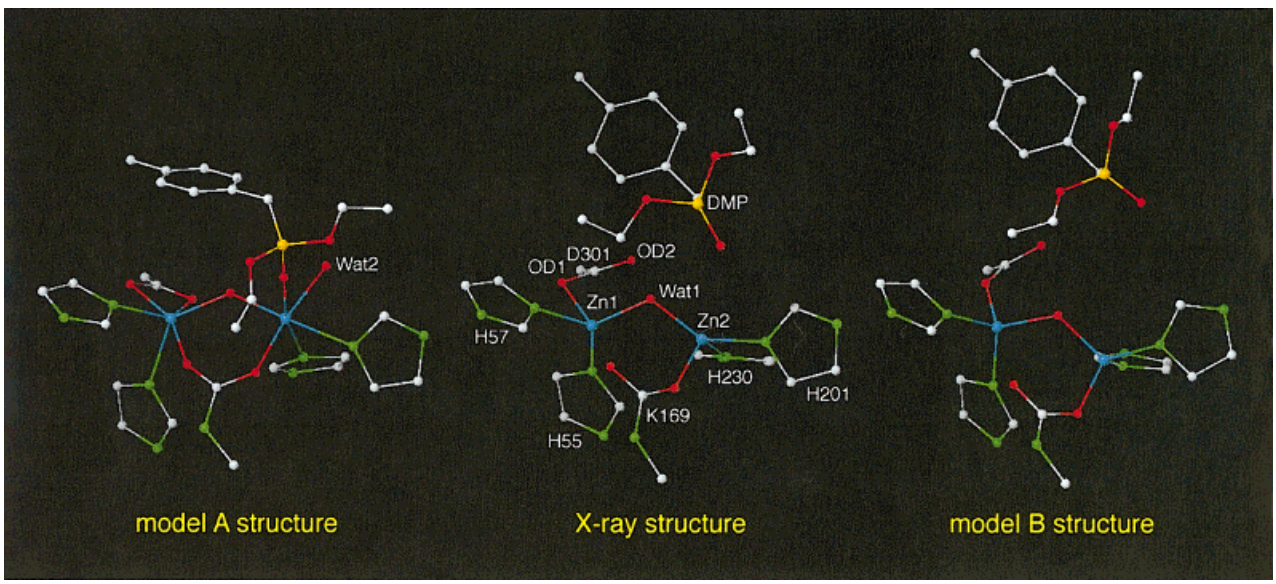

Fig. 2. Zinc complexes in the X-ray structure and in the time-average structures simulated using model A for 600 ps and model B for 2.0 ns, respectively (green = N; white = C; red = O; yellow = P; and cyan = Zn).

TABLE I. Atom Types and the RESP Charges of DMP[†]

Atom id	Atom type	RESP charge (e)
1	HC	0.061
2	CT	−0.1824
3	HC	0.061
4	HC	0.061
5	CA	0.1111
6	CA	−0.1749
7	HA	0.1397
8	CA	−0.1965
9	HA	0.1535
10	CA	0.0058
11	CA	−0.1965
12	HA	0.1535
13	CA	−0.1749
14	HA	0.1397
15	CT	−0.1577
16	HC	0.0998
17	HC	0.0998
18	P	0.8601
19	O	−0.6401
20	OS	−0.3566
21	CT	0.0805
22	H1	0.0605
23	H1	0.0605
24	CT	−0.0431
25	HC	0.0289
26	HC	0.0289
27	HC	0.0289
28	OS	−0.3566
29	CT	0.0805
30	H1	0.0605
31	H1	0.0605
32	CT	−0.0431
33	HC	0.0289
34	HC	0.0289
35	HC	0.0289

[†]For atom ids, see Figure 5.

TABLE II. Atom Types and the RESP Charges of the Carbamylated Lysine[†]

Atom id	Atom type	RESP charge (e)
1	N	−0.3808
2	H	0.2722
3	CT	−0.0637
4	H1	0.0487
5	CT	0.0153
6	HC	0.02
7	HC	0.02
8	CT	−0.1343
9	HC	0.0378
10	HC	0.0378
11	CT	−0.0766
12	HC	0.0254
13	HC	0.0254
14	CT	0.3692
15	HP	−0.0379
16	HP	−0.0379
17	N2	−0.8693
18	H	0.3223
19	C	0.9999
20	O2	−0.8297
21	O2	−0.8297
22	C	0.6053
23	O	−0.5392

[†]For atom ids, see Figure 5.

protonation states of other residues of PTE and Wat1 were the same as those assigned in the PTE structure with protonation of type I. The RESP charges of DMP and the carbamylated lysine (Lyx169) were generated according to the published protocol.[25] The RESP charges and the force field parameters of the two residues are provided in Tables I–III.

MD Simulations

All MD simulations were performed by employing the SANDER module of the AMBER 5.0 program[26] with the Cornell et al. force field[27] and additional force field parameters listed in Tables I–III. All MD simulations used

1. a dielectric constant of 1.0;
2. the Berendsen coupling algorithm[28];
3. a periodic boundary condition in the NPT ensemble at constant temperature of 298K (or 300K, as reported by Zhan et al.[22]) and constant pressure of 1 atm with isotropic molecule-based scaling;
4. the Particle Mesh Ewald (PME) method to calculate the long-range electrostatic interactions;[29]
5. a weak harmonic restraint in the Cartesian space with a force constant of 0.01 kcal/(mol*Å^2) applied to Na^+, Cl^- and the 67 crystallographically determined water molecules, not including the zinc ions and hydroxide, to avoid potential interruptions of the simulation caused by excessively large separations of these small molecules, which were treated as "solute" molecules, from the protein; and
6. default values of all other inputs of the SANDER module.

By employing the EDIT module, the DMP-PTE complex structure was solvated with either 10,878 TIP3P water molecules[30] (solvation of type I: NCUBE = 20, QH = 0.4170, DISO = 2.20, DISH = 2.00, CUTX = 10.0, CUTY = 11.0, and CUTZ = 12.5) or 7,927 water molecules (solvation of type II: NCUBE = 20, QH = 0.4170, DISO = 2.20, DISH = 2.00, CUTX = CUTY = CUTZ = 8.2) including two zinc ions, one hydroxide, Na^+ ions, Cl^- ions, and the 67 crystallographically determined water molecules. Solvation of type I was an approximation of the simulation condition reported by Zhan et al.[22] PME setups of types I and II (type I: BOXX = 74.6572, BOXY = 73.7330, BOXZ = 74.3263, ALPHA = BETA = GAMMA = 90.0, NFFTX = 64, NFFTY = 64, NFFTZ = 64, SPLINE_ORDER = 4, ISCHARGED = 0, EXACT_EWALD = 0, and DSUM_TOL = 0.00001; type II: BOXX = 71.0569, BOXY = 68.1264, BOXZ = 65.7165, ALPHA = BETA = GAMMA = 90.0, NFFTX = 64, NFFTY = 64, NFFTZ = 64, SPLINE_ORDER = 4, ISCHARGED = 0, EXACT_EWALD = 0, and DSUM_TOL = 0.00001) were used for solvation of types I and II, respectively. The resulting system consisted of

TABLE III. Force Field Parameters of Zinc Divalent Cation (ZN), Dummy Atom (DZ), DMP, and the Carbamylated Lysine

Bond	K [kcal/mol Å^2]	R_{eq} (Å)
CT-P	230	1.61
P-O	525	1.48
N2-C	481	1.34
DZ-ZN	540	0.90
DZ-DZ	540	1.470

Angle	K [kcal/mol radian^2)]	T_{eq} (deg.)
CA-CT-P	100	120.5
HC-CT-P	100	120.5
CT-P-OS	100	108.23
CT-N2-C	50	123.2
N2-C-O2	70	120
H-N2-C	35	120
CT-P-O	100	108.23
O-P-OS	100	108.23
DZ-ZN-DZ	55	109.50
DZ-DZ-DZ	55	60.0
DZ-DZ-ZN	55	35.25

Dihedral	IDIVF	V_n/2 (kcal/mol)	γ (deg.)	N
X-CT-P-X	3	0.75	0	3
X-N2-C-X	4	9.6	180	2
ZN-DZ-DZ-DZ	1	0	35.3	2
DZ-ZN-DZ-DZ	1	0	120.0	2
DZ-DZ-DZ-DZ	1	0	70.5	2

Improper dihedral	V_n/2 (kcal/mol)	γ (deg.)	N
X-X-CA-CA	1.1	180	2

VDW	Mass	R* (Å)	Eps (kcal/mol)	VDW	Mass	R* (Å)	Eps (kcal/mol)
ZN	53.38	3.1	1E-6	DZ	3.0	0	0

37,722 (solvation of type I and protonation of type II), 37,716 (solvation of type I and protonation of type I), or 28,817 (solvation of type II and protonation of type II) atoms. Such systems were first energy minimized for 500 steps to remove close van der Waals contacts in the system. The minimized systems were then slowly heated to 298 or 300 K (10K/ps) and equilibrated for 100 ps before simulation.

Five different model A-based MD simulations were carried out in order to demonstrate that the problem of model A is not caused by the different use of the SHAKE algorithm or by the use of different methods of solvation and protonation. The first simulation used

1. a simulation of time of 600 ps;
2. a 2.0 fs time step;
3. the SHAKE algorithm[31] applied to all bonds containing hydrogen atom;
4. protonation of type I;
5. the non-bonded atom pair list updated at every 10 steps;
6. temperature at 300K; and
7. solvation of type I.

The second simulation used

1. a simulation time of 600 ps;
2. a 2.0 fs time step;
3. the SHAKE algorithm applied to all bonds containing hydrogen atom;
4. protonation of type II;
5. the non-bonded atom pair list updated at every 10 steps; and
6. solvation of type I.

The third simulation used

1. a simulation time of 600 ps;
2. a 2.0 fs time step;
3. the SHAKE algorithm applied to all bonds of the system;
4. protonation of type I;
5. the non-bonded atom pair list updated at every 10 steps; and
6. solvation of type II.

The fourth simulation used

1. a simulation time of 2.0 ns;
2. a 2.0 fs time step;
3. the SHAKE algorithm applied to all bonds of the system;
4. protonation of type II;

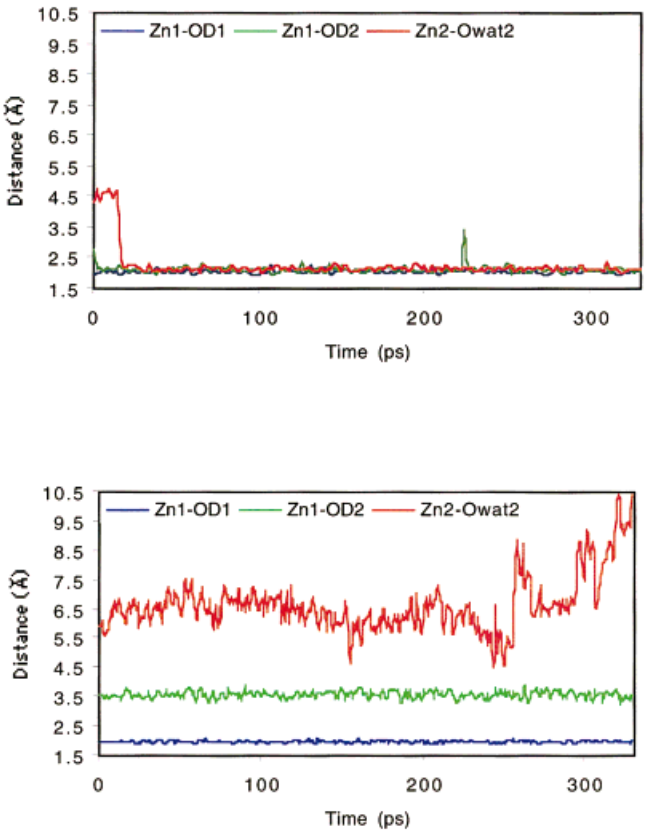

Fig. 3. Distances of Zn^{2+} to the carboxyl O atoms of D301 and to the O atom of Wat2, which were obtained from the first Model A simulation (top) and the second Model B simulation (bottom), respectively.

5. the non-bonded atom pair list updated at every 10 steps; and
6. solvation of type II.

The fifth simulation used

1. a simulation time of 1.0 ns;
2. a 1.0 fs time step;
3. the SHAKE algorithm applied to all bonds of the system;
4. protonation of type I;
5. the non-bonded atom pair list updated at every 20 steps; and
6. solvation of type II.

Two different model B-based MD simulations were performed to demonstrate that the success of model B is not affected by the different use of the SHAKE algorithm or by the use of different mass of the cationic dummy atom. All these simulations used

1. a simulation of 2.0 ns;
2. a 1.0 fs time step;
3. protonation of type II;
4. the non-bonded atom pair list updated at every 20 steps; and

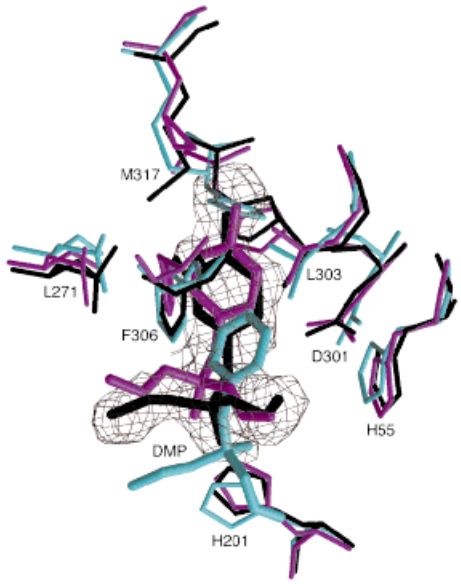

Fig. 4. The F_O–F_c map at 3.0 σ around DMP (thin stick model) in the X-ray structure of PTE (black) and the time-average structures of PTE derived from the 2.0 ns MD simulations using models A (cyan) and B (magenta), respectively.

5. solvation of type II.

The first simulation used

1. the SHAKE algorithm applied to all bonds of the system; and
2. 0.1 as the mass of the cationic dummy atom and 65.380 as the mass of the zinc atom.

The second simulation used

1. the SHAKE algorithm applied to all bonds involving hydrogen atom; and
2. 3.0 as the mass of the cationic dummy atom and 53.380 as the mass of the zinc atom.

The RMSDs were calculated by a mass-weighted fitting of the two complexes using the CARNAL module of the AMBER 5.0 program.

RESULTS AND DISCUSSION

A 600 ps (2.0 fs time step) MD simulation of the DMP-PTE complex was first performed using model A with the CHARMM force field parameters for Zn^{2+} (ϵ = 0.25 kcal/mol, r* = 1.09 Å, and the atomic charge of zinc ion is "+2")[14] that were reportedly adaptable to the simulation of the DMP-PTE complex with the AMBER 95 force field.[22] The 600 ps simulation was carried out in accordance with the reported 550 ps MD simulation of the DMP-PTE complex.[22] The root-mean-square deviations (RMSDs) for the DMP, PTE, and their complex between the X-ray structure and the time-average structure of the 600 ps MD simulation were 2.49, 1.00, and 1.02 Å, respectively, indicating a significant displacement in the

position of DMP as compared to the X-ray structure. Although all the reported distances (Zn1-O^{Wat1} = 2.0 Å, Zn2-O^{Wat1} = 2.0 Å, and Zn1-Zn2 = 3.6 Å, Fig. 2) calculated from the 550 ps MD simulation using model A[22] were identical to the distances calculated from the time-average structure of the 600 ps MD simulation using model A, a substantial difference of the active site between the X-ray structure and the time-average structure from the 600 ps MD simulation was observed. In the X-ray structure, one zinc ion (Zn1) was coordinating to only one carboxyl oxygen atom (Zn1-OD1 = 2.4 Å and Zn1-OD2 = 3.2 Å) of D301 (Fig. 2). In the time-average and all the instantaneous structures of the 600 ps MD simulation (Figs. 2,3), Zn1 was coordinating to two carboxyl oxygen atoms (Zn1-OD1 = 2.1 Å and Zn1-OD2 = 2.2 Å) of D301. Similarly, two carboxyl oxygen atoms of the carbamylated lysine 169 in the X-ray structure were not coordinating to Zn1, but one of them became a coordinate of Zn1 during the 600 ps MD simulation thereby converting the four-ligand coordination of Zn1 identified in the X-ray structure to six-ligand coordination (Fig. 2). In addition, one oxygen atom of DMP, that was 3.46 Å away from another zinc ion (Zn2) in the X-ray structure, was coordinating with Zn2 at a separation of 2.1 Å in the time-average structure of the 600 ps MD simulation (Fig. 2). Furthermore, one water molecule (Wat2), that was initially 4.4 Å away from Zn2, crept toward Zn2 and was kept at a distance of 2.0 Å from Zn2 during the entire 600 ps MD simulation (Fig. 3). The four-ligand coordination of Zn2 identified in the X-ray structure was thus converted to six-ligand coordination in the model A-based MD simulation (Fig. 2). This striking difference in the active site between the X-ray and MD structures, which was not described in the report of the 550 ps MD simulation,[22] was confirmed by five different MD simulations using model A one of which was a 2.0 ns MD simulation (see Methods).

A 2.0 ns (1.0 fs time step) MD simulation of the DMP-PTE complex was then carried out using model B.[18] The distance between the two *heavy* zinc ions in the time-average structure of the model B-based 2.0 ns MD simulation and the X-ray structure was 3.39 ± 0.07 (2,000) Å and 3.31 ± 0.001 (2) Å, respectively, in contrast to the corresponding distance of 3.64 ± 0.06 (1,000) Å in the 2.0 ns MD simulation using model A. This result provides evidence of the accuracy of model B in terms of the force field parameters for the zinc–zinc interaction. The four-ligand coordination for the two zinc ions identified in the X-ray structure were maintained throughout the 2.0 ns MD simulation (Figs. 2,3).

Consistent with the X-ray structure, Zn1 in the time-average and all the instantaneous MD structures was coordinating to only one carboxyl oxygen atom (Zn1-OD1 = 2.0 Å and Zn1-OD2 = 3.6 Å) of D301. Only one water molecule (Wat1) was coordinating to Zn1 and Zn2 during the entire 2.0 ns MD simulation using model B. The RMSDs of DMP, PTE, and their complex between the X-ray structure and the time-average structure of the 2.0 ns MD simulation were 0.89, 1.11, and 1.11 Å, respectively, indicating the time-average structure of the simulation using model B was essentially identical to the X-ray structure at the resolution of 2.1 Å.[23] Unequivocally, fitting the time-average structures of the PTE complex simulated using models A and B for 2.0 ns, respectively, into the difference electron density map of the PTE X-ray structure with DMP omitted revealed that only the model B-based MD structure was able to fit into the density map (Fig. 4). The result of the MD simulation using model B was confirmed by another model B-based 2.0 ns (1.0 fs time step) MD simulation using different conditions as described in Methods.

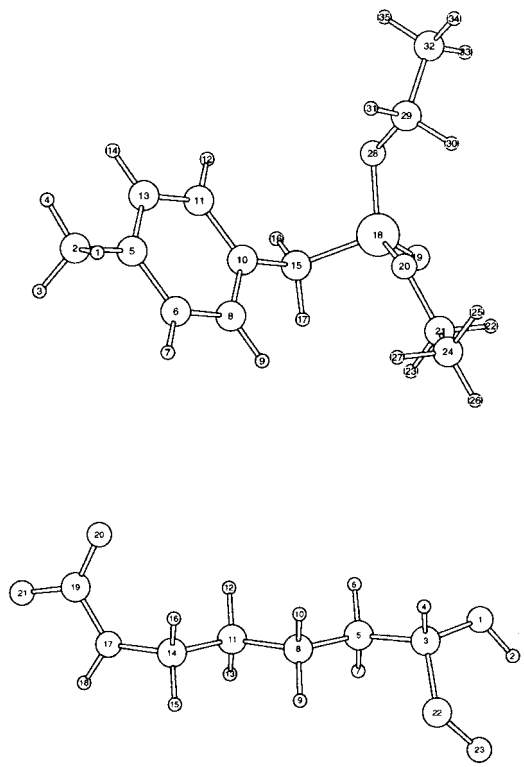

Fig. 5. The 3D structures of DMP and the carbamylated lysine showing atom ids.

The present study demonstrates that one can successfully simulate not only the four-ligand coordination of zinc in proteins but also the interatomic distance between two nearby zinc ions in proteins using the cationic dummy atom approach. The results suggest that caution should be used in the MD simulations using the nonbonded method. Furthermore, the present work supports the notion of using cationic dummy atoms to mimic vacant orbitals of metal ions that accommodate the lone-pair electrons of the metallic ligands thus imposing the requisite orientational requirement for the ligands. It offers an incentive to use cationic dummy atoms to effectively model the atomic structures of many biologically important metalloproteins that represent one third of known proteins.

CONCLUSION

The cationic dummy atom method was able to simulate the four-ligand coordination of two zinc complexes that

was bridged by a hydroxide in PTE. The distance (3.39 ± 0.07Å) between two nearby zinc ions in the time-average structure of PTE derived from the MD simulation using the cationic dummy atoms matched that in the X-ray structure (3.31 ± 0.001Å). Unequivocally, the time-average structure of PTE was able to fit into the experimentally determined difference electron density map of the corresponding X-ray structure. The results demonstrate the practicality of the cationic dummy atom method for MD simulations of zinc proteins bound with multiple zinc ions. In contrast, a 2.0 ns (1.0 fs time step) MD simulation using the nonbonded method revealed a striking difference in the active site between the X-ray structure and the time-average structure that was unable to fit into the density map of PTE. The results suggest that caution should be used in the MD simulations using the nonbonded method.

ACKNOWLEDGMENTS

I thank H. M. Holden for providing the structure factor file of the PTE complex, and J.L. Sussman and M. Harel for crystallographic analysis of the DMP-PTE structures derived from the MD simulations.

REFERENCES

1. Mackay JP, Crossley M. Zinc fingers are sticking together. Trends Biochem Sci 1998;23:1–4.
2. Boehm T, Oreilly MS, Keough K, Shiloach J, Shapiro R, Folkman J. Zinc-binding of endostatin is essential for its antiangiogenic activity. Biochem Biophys Res Commun 1998;252:190–194.
3. Hanahan D, Folkman J. Patterns and emerging mechanisms of the angiogenic switch during tumorigenesis. Cell 1996; 86:353–364.
4. Vu TH, Shipley JM, Bergers G, Berger JE, Helms JA, Hanahan D, Shapiro SD, Senior RM, Werb Z. Mmp-9/gelatinase B is a key regulator of growth plate angiogenesis and apoptosis of hypertrophic chondrocytes. Cell 1998;93:411–422.
5. Santos O, McDermott CD, Daniels RG, Appelt K. Rodent pharmacokinetic and anti-tumor efficacy studies with a series of synthetic inhibitors of matrix metalloproteinases. Clin Exp Metastasis 1997;15:499–508.
6. Klimpel KR, Arora N, Leppla SH. Anthrax toxin lethal factor contains a zinc metalloprotease consensus sequence which is required for lethal toxin activity. Mol Microbiol 1994;13:1093–100.
7. Atassi MZ, Oshima M. Structure, activity, and immune (T and B cell) recognition of botulinum neurotoxins. Crit Rev Immunol 1999;19:219–260.
8. Pang YP, Xu K, El Yazal J, Prendergast FG. Successful molecular dynamics simulation of the zinc-bound farnesyltransferase using the cationic dummy atom approach. Protein Sci 2000; 9:1857–1865.
9. Hoops SC, Anderson KW, Merz KMJ. Force field design for metalloproteins. J Am Chem Soc 1991;113:8262–8270.
10. Ryde U. Molecular dynamics simulations of alcohol dehydrogenase with a four- or five-coordinate catalytic zinc ion. Proteins 1995;21:40–56.
11. Lu DS, Voth GA. Molecular dynamics simulations of human carbonic anhydrase II: Insight into experimental results and the role of solvation. Proteins 1998;33:119–134.
12. Vedani A, Huhta DW. A new force field for modeling metalloproteins. J Am Chem Soc 1990;112:4759–4767.
13. Aqvist J, Warshel A. Computer simulation of the initial proton transfer step in human carbonic anhydrase I. J Mol Biol 1992;224: 7–14.
14. Stote RH, Karplus M. Zinc binding in proteins and solution: a simple but accurate nonbonded representation. Proteins 1995;23: 12–31.
15. Wasserman ZR, Hodge CN. Fitting an inhibitor into the active site of thermolysin: a molecular dynamics case study. Proteins 1996;24: 227–37.
16. Donini OAT, Kollman PA. Calculation and prediction of binding free energies for the matrix metalloproteinases. J Med Chem 2000;43:4180–4188.
17. Berweger CD, Thiel W, van Gunsteren WF. Molecular-dynamics simulation of the beta domain of metallothionein with a semi-empirical treatment of the metal core. Proteins 2000;41:299–315.
18. Pang YP. Novel zinc protein molecular dynamics simulations: Steps toward antiangiogenesis for cancer treatment. J Mol Model 1999; 5:196–202.
19. Aqvist J, Warshel A. Free energy relationships in metalloenzyme-catalyzed reactions. Calculations of the effects of metal ion substitutions in staphylococcal nuclease. J Am Chem Soc 1990;112: 2860–2868.
20. Roe RR, Pang YP. Zinc's exclusive tetrahedral coordination governed by its electronic structure. J Mol Model 1999;5:134–140.
21. ElYazal J, Pang YP. Ab initio calculations of proton dissociation energies of zinc ligands: Hypothesis of imidazolate as zinc ligand in proteins. J Phys Chem B 1999;103:8773–8779.
22. Zhan CG, de Souza ON, Rittenhouse R, Ornstein RL. Determination of two structural forms of catalytic bridging ligand in zinc-phosphotriesterase by molecular dynamics simulation and quantum chemical calculation. J Am Chem Soc 1999;121:7279–7282.
23. Vanhooke JL, Benning MM, Raushel FM, Holden HM. Three-dimensional structure of the zinc-containing phosphotriesterase with the bound substrate analog diethyl 4-methylbenzylphosphonate. Biochemistry 1996;35:6020–6025.
24. ElYazal J, Roe RR, Pang YP. Zinc's affect on proton transfer between imidazole and acetate predicted by large basis set ab initio calculations. J Phys Chem B 2000;104:6662–6667.
25. Cieplak P, Cornell WD, Bayly C, Kollman PA. Application of the multimolecule and multiconformational resp methodology to biopolymers: charge derivation for DNA, RNA, and proteins. J Comp Chem 1995;16:1357–1377.
26. Pearlman DA, Case DA, Caldwell JW, Ross WS, Cheatham III TE, Debolt S, Ferguson D, Seibel G, Kollman PA. AMBER, a package of computer programs for applying molecular mechanics, normal mode analysis, molecular dynamics and free energy calculations to simulate the structural and energetic properties of molecules. Comput Phys Commun 1995;91:1–41.
27. Cornell WD, Cieplak P, Bayly CI, Gould IR, Merz Jr. KM, Ferguson DM, Spellmeyer DC, Fox T, Caldwell JW, Kollman PA. A second generation force field for the simulation of proteins, nucleic acids, and organic molecules. J Am Chem Soc 1995;117: 5179–5197.
28. Berendsen HJC, Postma JPM, van Gunsteren WF, Di Nola A, Haak JR. Molecular dynamics with coupling to an external bath. J Chem Phys 1984;81:3684–3690.
29. Darden TA, York DM, Pedersen LG. Particle Mesh Ewald: An N log(N) method for Ewald sums in large systems. J Chem Phys 1993;98:10089–10092.
30. Jorgensen WL, Chandreskhar J, Madura JD, Impey RW, Klein ML. Comparison of simple potential functions for simulating liquid water. J Chem Phys 1982;79:926–935.
31. Ryckaert JP, Ciccotti G, Berendsen HJC. Numerical integration of the Cartesian equations of motion of a system with constrains: molecular dynamics of n-alkanes. J Comput Phys 1977;23:327–341.